Pulse Optimization and Control of Quantum Cascade Laser via an All-Optical Approach

Chen Peng, Haijun Zhou, Liguo Zhu, Tao Chen, Lianghui Du, Yu Zhu, Yi Zou, Qixian Peng, Gang Chen, *Member, IEEE*, and Zeren Li

***Abstract*— Pulse optimization and control are demonstrated in a standard middle-infrared quantum cascade laser by illuminating its front facet with two near-infrared lasers. The 1550- and 850-nm near-infrared lasers are used to optimize the pulse rise/fall time and the pulse shape, respectively, of the quantum cascade laser. Compared with the electric drive, the electron interband transition is directed by the all-optical approach. Simultaneously, the quantum cascade laser's pulse width, amplitude, and repetition rate are controlled precisely by changing the two near-infrared lasers' delay time, average power, and repetition rate. Such an all-optical approach is beneficial in the high-speed optimization and control of the quantum cascade laser pulse. It has the potential for application in free-space optical communication and high-speed frequency modulation spectroscopy.**

***Index Terms*— All-optical modulation, quantum cascade laser, high-speed frequency modulation.**

I. Introduction

As A unipolar mid-infrared laser source, the quantum cascade laser (QCL) [1] was invented at Bell Labs over two decades ago. It has attracted wide attention in free-space optical communication (FSOC) and trace gas detection applications [2], [3]. High-speed frequency modulation of QCLs can improve the data transmission in FSOC and sensitivity in gas detection [4]–[6]. Compared with thermal modulation and electrical modulation of QCLs, the all-optical approach allows a modulation bandwidth up to 100 GHz in theory due to the influence of the parasitic capacitance effect [7]. Recently, S. Suchalkin reported an improved performance in terms of the modulation bandwidth (up to 20 GHz) by illuminating the whole waveguide with 1.3 μm near-infrared (NIR) light [8]. When the QCLs work in pulse mode, the pulse shape and quality of QCLs are important for the applications in high-speed frequency modulation. Therefore, these parameters of QCLs' pulse, including pulse rise/fall time, pulse width and pulse shape affect the signal fidelity and effective signal rate. They are necessary to be optimized. Usually, the laser design, modulation parameters, and laser working environment need to be considered in the optimization, which is not only complicated but also difficult to control accurately. In this letter, we demonstrated the pulse optimization of QCLs via an all-optical approach, which can control the pulse parameters efficiently with high speed.

When QCLs are operated with a pulsed current above the threshold, the electron interband transition in the active region is governed by the injection current. Therefore, the pulse rise time depends on the speed of the electrode injection current. However, there are inductance, capacitance and current injection electrode, which will prolong the rise and fall time of the QCL pulse. The all-optical approach is used to illuminate the active region facet of the QCL with an NIR laser [9], and the electron interband transition in the active region is directed by the external light excitation. It changes the carrier distribution at the subband rapidly, and then achieves high modulation speed. Theoretically, due to the fast electron relaxation, as fast as tens of picoseconds [10], an ultra-short pulse rise time is achieved. This approach has been verified to a ns level [11]. Recently, researchers demonstrated that if an NIR laser at different wavelengths was used to modulate the QCL, it would cause different QCL's amplitude fluctuations [12]. It is determined by photon energy and electron temperature [13], [14]. Therefore, we can use two optimized NIR lasers to realize high-speed regulation of the QCL rise/fall time. Moreover, the all-optical approach can excite electrons in the active region simultaneously and uniformly, so that the QCL pulse waveform is smooth. We can also use the all-optical approach to optimize the QCL pulse form.

II. Experimental Setup

Figure 1 shows the schematic diagram of the experimental setup. The QCL used in this experiment is the standard type I $Ga_{0.47}In_{0.53}AS/Al_{0.62}Ga_{0.38}As$ four-level Fabry-Perot QCL based on the two-phonon resonant design, with a central wavelength of 4.6 μm and a 2 μm thick core region, patterned in a cavity size of 15 μm (ridge width) $\times$ 1.358 mm (cavity length). It was mounted on a copper heat sink inside a liquid nitrogen cryostat (Janis VPF) and held at a temperature

Manuscript received January 23, 2018; revised April 18, 2018; accepted May 1, 2018. Date of publication May 4, 2018; date of current version May 22, 2018. This work was supported in part by the National Natural Science Foundation of China under Grant 61177093, Grant 61077057, in part by the Institute of Fluid Physics Foundation under Grant 052430, and in part by the China Post-Doctoral Science Foundation under Grant 2018M633408. *(Corresponding author: Zeren Li.)*

C. Peng, L. Zhu, T. Chen, L. Du, Y. Zhu, Y. Zou, Q. Peng, and Z. Li are with the Institute of Fluid Physics, China Academy of Engineering Physics, Mianyang 621900, China (e-mail: zeren109@yeah.net).

H. Zhou and G. Chen are with the Key Laboratory of Optoelectronic Technology & Systems, Ministry of Education, Chongqing University, Chongqing 400044, China.

Color versions of one or more of the figures in this letter are available online at http://ieeexplore.ieee.org.

Digital Object Identifier 10.1109/LPT.2018.2833169

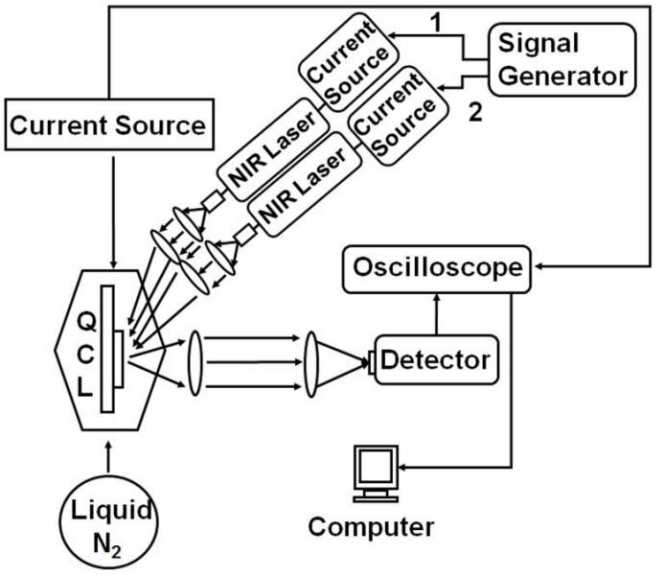

Fig. 1. Experimental setup of the two NIR lasers exciting a QCL based on the all-optical approach.

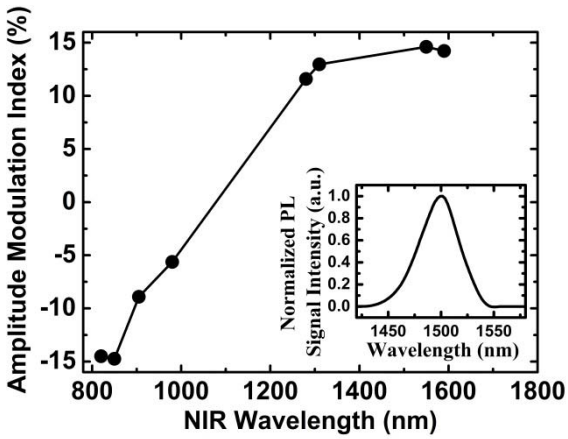

Fig. 2. Change in QCL amplitude modulation index vs. NIR wavelength; the inset shows the (PL) spectrum by directly illuminating the front facet of the QCL with an 820 nm beam.

of 80 K, and we utilized a current source (ILX Lightwave LDP 3811) to drive it. Using two CaF_2 lenses, the QCL's MIR emission is collimated and then focused onto an infrared photovoltaic detector (Vigo PEMI-2TE-6). These NIR lasers are common semiconductor laser diodes (3 pin or 4 pin, which are mainly provided by Throlabs). Two semiconductor laser current sources are triggered by two pulse signals with the same amplitude, repetition frequency, and pulse width generated by a signal generator (Tektronix AWG 5014C). The phases of the two NIR beams can be controlled by adjusting the delay time of the two trigger pulse signals. Finally, the two NIR beams are focused onto the QCL front facet with an incident angle of approximately 30° to the QCL beam, and the NIR focal spot diameter is less than 20 μm. The NIR focal spot diameter was measured by knife-edge method with a Sigma 3D translation stage with a travel accuracy of 1μm.

III. Experimental Results and Discussion

To find the optimized excitation wavelengths for this NIR laser, we investigated the photoluminescence (PL) spectrum by directly illuminating the front facet of the QCL with an 820 nm beam while the DC bias current was at the threshold. The inset in figure 2 shows the PL spectrum peak at 1500 nm. It is proved that the photon energy of a 1500 nm NIR laser is closest to the band gap between the laser band and valence band of the QCL, which is most likely to lead to the electron interband transition. Furthermore, we use eight different NIR lasers emitted at wavelengths of 820 nm, 850 nm, 905 nm, 980 nm, 1280 nm, 1310 nm, 1550 nm, and 1590 nm to excite the QCL, and the average power of each NIR laser is 2 mW. The QCL is operated in pulse mode by a 10 kHz current pulse with a width of 200 ns. As shown in Figure 2, The QCL amplitude modulation index shows the two different groups of modulation. One group consists of the short-wavelength lasers (820 nm, 850 nm, 905 nm, and 980 nm) that lead to a reduction in the QCL pulse intensity, and where the 850 nm laser induces the most pronounced reduction of −14.74 %. The other group consists of the long-wavelength lasers (1280 nm, 1310 nm, 1550 nm, and 1590 nm) that conversely lead to an increase in the QCL pulse intensity. The 1550 nm laser induces an amplitude modulation index of 14.61 %, which is greater than that induced by the others. These two different modulations could be used to optimize the rise and fall times of the QCL pulses, respectively. It is worth mentioning that the relationship between the NIR wavelengths and QCL pulse intensity changes is not perfectly proportional. For example, the 1590 nm laser induces an amplitude modulation index of QCL is less than 1550 nm laser. This is due to lower energy leading to a decrease in the number of electrons in the interband transition. Further, the 820 nm laser induces an amplitude modulation index of QCL that is less than that of the 850 nm laser as well, because a higher energy causes electrons to be excited to a higher subband and does not contribute to modulation. Therefore, the 1550 nm and the 850 nm lasers have the highest positive and negative amplitude modulation index of QCL, so they are optimized. Here, we utilize them in the following experiments.

To protect the QCL from damage, we use low power NIR lasers to modulate the QCL. We let the QCL work near the threshold current and ensure that there is no emission. Simultaneously, a 1550 nm beam with an average power of approximately up to 3 mW is focused onto the facet of the active region of the QCL. The rise time of the two pulse signals triggering the two NIR semiconductor laser current are less than 1ns. Since the long wavelength NIR lasers could lead to an increase in the QCL pulse intensity, the ultra-short QCL pulse rise time can be achieved by the all-optical approach. Rise time is the time taken by a signal to change from a specified low value to a specified high value, which are commonly the 10% and 90% of the output stepheight [15]. We recorded the time of the QCL pulse signal generated by the electric drive and the all-optical modulation from zero up to the peak steadily. We also normalized the intensity of the QCL pulse signal for facilitating the comparison. As shown

in figure 3(a), the rise time of a QCL pulse with a width of 200 ns, which is generated by the electric drive, is 29.6 ns, and that generated by the all-optical modulation is only 7.1 ns. Because the highest response time of our detection circuitry is about 2 ns, and the QCL does not have specially designed optical injection window. All these will affect the rise/fall time of the experiment. So the experimental results with all-optical modulation approach are not consistent with the theory. However, compared to the electric drive approach, the rise time is shortened by 3/4, which is a significant improvement. Similarly, the short-wavelength NIR lasers could lead to a reduction in the QCL pulse intensity; the QCL pulse fall time can be optimized by the all-optical approach. We utilized an 850 nm beam with an average power of approximately 2.6 mW to suppress the QCL pulse completely. The powers of the 850 nm and 1550 nm NIR lasers are not matched very well, because when the total power of NIR illumination increases, the amount of energy obtained per unit area of the QCL front facet also increases, which causes the lattice temperature of the QCL to rise. Thus, the QCL's threshold current rises and output power decreases. As shown in figure 3(b), the fall time of a QCL pulse with a width of 200 ns, which is generated by the electric drive and all-optical approach, is 24.7 ns and 15.8 ns, respectively. The fall time is shortened by 2/5. Compared with the 1550 nm laser, the 850 nm laser, for which the photon energy is much greater than the subband edge, the excess energy excites the electron to a higher level or the high k state, resulting in a larger number of hot carriers [14]. Hot carriers relax through electron-electron scattering, convert the excess energy into heat, increase the electron temperature, and decrease the QCL optical emission rate. That process is not direct, and it prolongs the fall time. However, the fall time can also be optimized by the all-optical approach. In addition, we determined that the QCL pulse generated by all-optical modulation is smoother. This is due to the direct modulation of the electron transition by the all-optical modulation, and the QCL pulses are mainly affected by the quality of the NIR laser, not by other factors.

In order to further optimize the pulse rise/fall time for this QCL, we observed the QCL pulse rise/fall time in different injection currents. A 1550 nm beam with an average power of approximately 3 mW is focused onto the facet of the active region of the QCL. As shown in Fig. 4, when the injection current is less than 185 mA, the QCL hasn't emission. The QCL pulse rise time has a small reduction (1 ns) until the injection current up to the threshold. This is because more optical energy has been increased the carrier concentration of the lasing subband in the active region of the QCL. When the injection current keeps on increasing, the QCL pulse rise time increases rapidly and tends to be stable. Because the modulation is switched from all-optical modulation to electric drive rapidly. However, the QCL pulse fall time has a small increment (2.3 ns) until the injection current up to the threshold. This is because more optical energy needs to suppress the amplitude modulation of the QCL. When the injection current keeps on increasing, the QCL pulse fall time increases rapidly and tends to be stable. Because the modulation is switched from all-optical modulation to electric

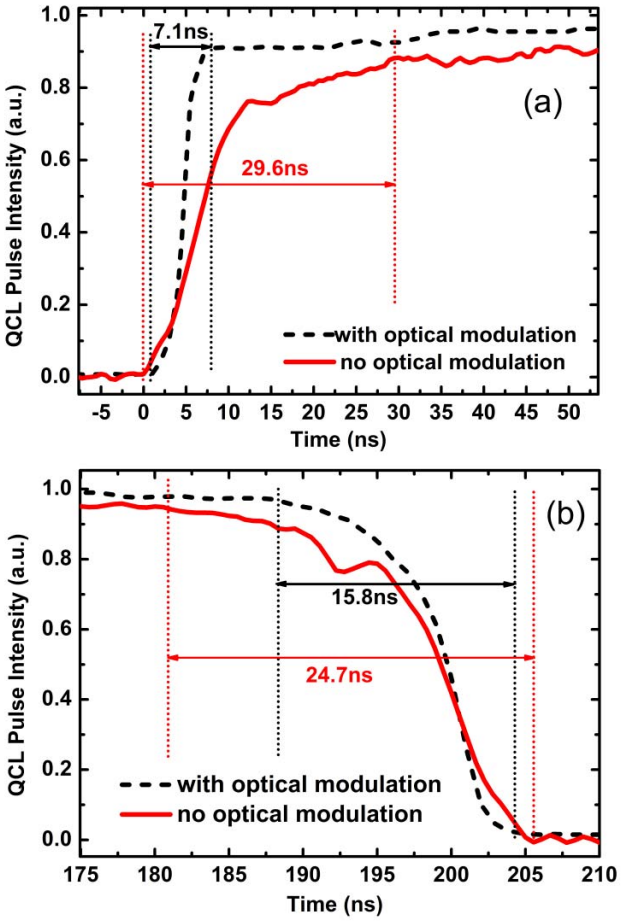

Fig. 3. (a) QCL pulse generated in the rise time by an electric drive (solid) and with 1550 nm NIR modulation (dash), (b) QCL pulse generated in the fall time by an electric drive (solid) and with 850 nm NIR modulation (dash).

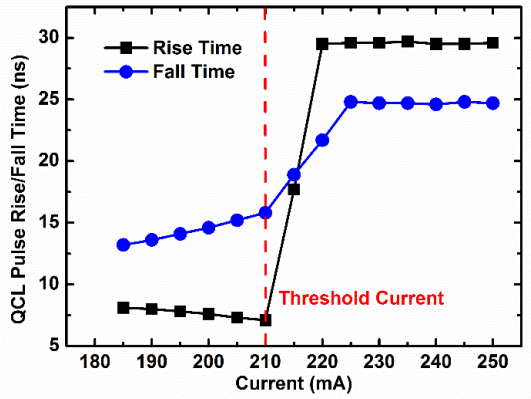

Fig. 4. QCL pulse rise (square)/fall (circle) time with different electric drives.

drive too. We find that when the injection current is close to or at the threshold, the rise/fall time is shorter, which is conductive to the optimization of QCL pulse by all-optical approach.

The all-optical modulation approach can not only optimize the rising/falling time and QCL pulse waveform but also control the QCL pulse width, amplitude, and repetition frequency in a certain range. This control is easy to implement

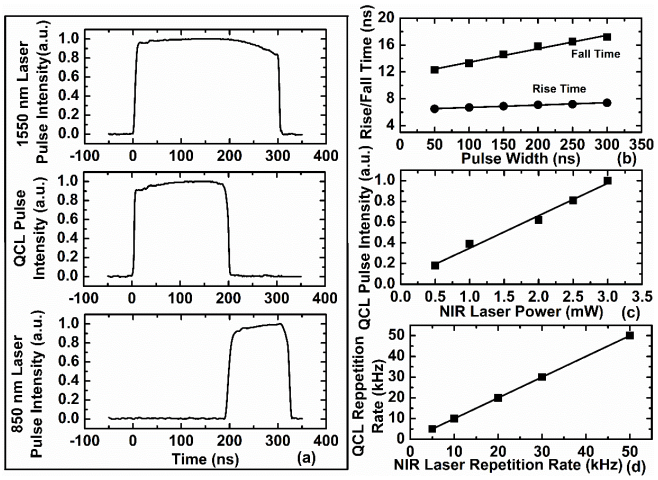

Fig. 5. (a) QCL pulse width was controlled by the modulation of two NIR lasers, (b) rise (circle)/fall (square) time vs. QCL pulse width, (c) QCL pulse intensity vs. NIR laser power, (d) QCL repetition rate vs. NIR laser repetition rate.

without affecting the optimization of the QCL pulse. The pulse width of the QCL pulse can be accurately controlled by the phase delay time of the two NIR lasers used for modulation. As shown in Fig. 5 (a), 1550 nm and 850 nm NIR lasers are used to control the opening and closing of the QCL pulse, respectively. The phase delay of two NIR lasers is controlled by a signal generator, and the phase delay is basically consistent with the QCL pulse width. The delay of the two NIR lasers in figure 5(a) is 200 ns, while the QCL pulse width is 202 ns. The pulse width of the QCL also affects the rising/falling times of the QCL pulse in a certain range. As shown in Figure 5 (b), as the pulse width of the QCL increases, the rise and fall times of the QCL have a similar linear increase. In the pulse range of 300 ns, the rise time increased by 0.9 ns, while the fall time increased by 4.9 ns. This is because with the accumulation of photon injection, the electron temperature of the QCL rises and the QCL's closing time is prolonged. Figure 5 (c) shows that by changing the average power of the NIR laser, the pulse intensity of the QCL can be adjusted without affecting the rise/fall time of the QCL pulse. Figure 5 (d) describes the relationship between the QCL pulse repetition rate and the NIR laser repetition rate, both of which are basically the same. Therefore, the QCL pulse can be controlled accurately and with high speed by controlling the two NIR lasers.

IV. Conclusion

In conclusion, the pulse optimization and control of the QCL with an all-optical approach is presented. It is based on positive and negative amplitude modulation of the QCL with different NIR excitation wavelengths. We used 1550 nm and 850 nm NIR lasers to optimize the QCL pulse rise/fall time and the pulse shape, respectively. Compared with the electric drive, the QCL pulse rise and fall times are shortened by 3/4 and 2/5, respectively, with the NIR lasers. And the rise/fall time improvement can be achieved only when operating the QCL close to or at the threshold current. Simultaneously, we can precisely adjust the QCL pulse width, amplitude, and repetition rate by changing the two NIR lasers' delay time, average power, and repetition rate. This all-optical approach can be used for the high-speed optimization and regulation of QCL pulses. In addition, it has the potential for FSOC and trace gas detection applications.

Acknowledgments

Chen Peng would like to thank Lei Gao at Chongqing University, Chongqing, China, for his helpful discussions. Gang Chen acknowledges the support of the NSFC. The authors are grateful to OSA Publishing Language Editing Services for its linguistic assistance during the preparation of this Letter.

References

[1] J. Faist, F. Capasso, D. L. Sivco, C. Sirtori, A. L. Hutchinson, and A. Y. Cho, "Quantum cascade laser," *Science*, vol. 264, no. 5158, pp. 553–556, 1994.

[2] C. Gmachl, F. Capasso, D. L. Sivco, and A. Y. Cho, "Recent progress in quantum cascade lasers and applications," *Rep. Progr. Phys.*, vol. 64, no. 11, pp. 1533–1601, 2001.

[3] G. Hancock, G. A. D. Ritchie, J.-P. H. Van Helden, D. Weidmann, and R. Walker, "Applications of midinfrared quantum cascade lasers to spectroscopy," *Opt. Eng.*, vol. 49, no. 11, p. 111121, 2010.

[4] P. Corrigan, R. Martini, E. A. Whittaker, and C. Bethea, "Quantum cascade lasers and the Kruse model in free space optical communication," *Opt. Exp.*, vol. 17, no. 6, pp. 4355–4359, 2009.

[5] T. Yang, C. Tian, G. Chen, and R. Martini, "Non-resonant optical modulation of quantum cascade laser and its application potential in infrared spectroscopy," *Proc. SPIE*, vol. 9002, p. 90021T, Feb. 2014.

[6] L. Dong *et al.*, "Compact TDLAS based sensor design using interband cascade lasers for mid-IR trace gas sensing," *Opt. Exp.*, vol. 24, no. 6, pp. A528–A535, 2016.

[7] F. Capasso, C. Gmachl, A. Tredicucci, A. L. Hutchinson, D. L. Sivco, and A. Y. Cho, "High performance quantum cascade lasers," *Opt. Photon. News*, vol. 10, no. 10, pp. 31–37, 1999.

[8] S. Suchalkin, G. Belenky, and M. A. Belkin, "Rapidly tunable quantum cascade lasers," *IEEE J. Sel. Topics Quantum Electron.*, vol. 21, no. 6, Nov./Dec. 2015, Art. no. 1200509.

[9] G. Chen, C. G. Bethea, and R. Martini, "Quantum cascade laser gain enhancement by front facet illumination," *Opt. Exp.*, vol. 17, no. 26, pp. 24282–24287, 2009.

[10] R. Paiella *et al.*, "High-speed operation of gain-switched midinfrared quantum cascade lasers," *Appl. Phys. Lett.*, vol. 75, no. 17, pp. 2536–2538, 1999.

[11] H. Cai *et al.*, "Femtosecond measurements of near-infrared pulse induced mid-infrared transmission modulation of quantum cascade lasers," *Appl. Phys. Lett.*, vol. 104, no. 21, p. 211101, 2014.

[12] T. Yang, G. Chen, C. Tian, and R. Martini, "Optical modulation of quantum cascade laser with optimized excitation wavelength," *Opt. Lett.*, vol. 38, no. 8, pp. 1200–1202, 2013.

[13] M. Elsässer, S. G. Hense, and M. Wegener, "Subpicosecond switch-off and switch-on of a semiconductor laser due to transient hot carrier effects," *Appl. Phys. Lett.*, vol. 70, no. 7, pp. 853–855, 1997.

[14] P. Harrison, D. Indjin, and R. W. Kelsall, "Electron temperature and mechanisms of hot carrier generation in quantum cascade lasers," *J. Appl. Phys.*, vol. 92, no. 11, pp. 6921–6923, 2002.

[15] E. M. Cherry and D. E. Hooper, *Amplifying Devices and Low-Pass Amplifier Design*. New York, NY, USA: Wiley, 1968.